OXFORD

Cerebral Cortex, 2023, **33**, 11526–11540
https://doi.org/10.1093/cercor/bhad385
Advance access publication date 17 October 2023
Original Article

Developmental plasticity of the structural network of the occipital cortex in congenital blindness

Saiyi Jiao[1], Ke Wang[1], Linjun Zhang[2], Yudan Luo[1], Junfeng Lin[1], Zaizhu Han[1,*]

[1]National Key Laboratory of Cognitive Neuroscience and Learning & IDG/McGovern Institute for Brain Research, Beijing Normal University, No. 19 Xinjiekouwai Street, Haidian District, Beijing 100875, China,
[2]School of Chinese as a Second Language, Peking University, No. 5 Yiheyuan Road, Haidian District, Beijing 100871, China

[*]Corresponding author: National Key Laboratory of Cognitive Neuroscience and Learning & IDG/McGovern Institute for Brain Research, Beijing Normal University, No. 19 Xinjiekouwai Street, Haidian District, Beijing 100875, China. Email: zzhhan@bnu.edu.cn

The occipital cortex is the visual processing center in the mammalian brain. An unanswered scientific question pertains to the impact of congenital visual deprivation on the development of various profiles within the occipital network. To address this issue, we recruited 30 congenitally blind participants (8 children and 22 adults) as well as 31 sighted participants (10 children and 21 adults). Our investigation focused on identifying the gray matter regions and white matter connections within the occipital cortex, alongside behavioral measures, that demonstrated different developmental patterns between blind and sighted individuals. We discovered significant developmental changes in the gray matter regions and white matter connections of the occipital cortex among blind individuals from childhood to adulthood, in comparison with sighted individuals. Moreover, some of these structures exhibited cognitive functional reorganization. Specifically, in blind adults, the posterior occipital regions (left calcarine fissure and right middle occipital gyrus) showed reorganization of tactile perception, and the forceps major tracts were reorganized for braille reading. These plastic changes in blind individuals may be attributed to experience-dependent neuronal apoptosis, pruning, and myelination. These findings provide valuable insights into the longitudinal neuroanatomical and cognitive functional plasticity of the occipital network following long-term visual deprivation.

Key words: occipital cortex; congenital blindness; cross-modal reorganization; longitudinal development.

Introduction

Brain plasticity refers to the remarkable ability of the brain to adapt to environmental constraints by reorganizing its gray and white matter tissues (Rakic 2002; Araneda et al. 2016). Acquired experiences play a powerful and sometimes invisible role in brain development (Greenough et al. 1987; Kolb 1998), driving plastic changes in both gray matter (Gaser and Schlaug 2003; Mechelli et al. 2004; Draganski et al. 2006) and white matter (Scholz et al. 2009; Wong et al. 2011; Sampaio-Baptista et al. 2013; McKenzie et al. 2014).

The occipital cortex, the location of the visual processing center in the brain, undergoes significant plastic reorganization in blind individuals following visual deprivation. These reorganizations involve changes in gray matter including reduced gray matter volume (GMV) in the bilateral primary visual cortex (Ptito et al. 2008; Bridge et al. 2009; Jiang et al. 2015), increased GMV in the lingual gyrus (LING) (Voss et al. 2014) and the left association visual cortex (Yang et al. 2014), and increased visual cortical thickness (Bridge et al. 2009; Jiang et al. 2009; Park et al. 2009; Voss and Zatorre 2012; Li et al. 2017). The reorganizations also extend to white matter, including reduced white matter volume (WMV) in the optic nerve, optic chiasm, optic radiation, geniculate cortex tract, inferior longitudinal fasciculus (ILF), and splenium of the corpus callosum (CC) (Noppeney et al. 2005; Shimony et al. 2006; Ptito et al. 2008; Park et al. 2009; Levin et al. 2010; Bock et al. 2013; Aguirre et al. 2016; Maller et al. 2016), increased WMV in the superior longitudinal fasciculus (SLF) (Ptito et al. 2008), decreased fractional anisotropy (FA) in the optic radiation, primary and ventral visual areas, ILF, SLF, inferior fronto-occipital fasciculus (IFOF) and splenium of the CC (Shimony et al. 2006; Yu et al. 2007; Bridge et al. 2009; Shu et al. 2009; Levin et al. 2010; Reislev et al. 2016) and increased diffusivity [e.g. mean diffusivity (MD) and radial diffusivity (RD)] in the splenium of the CC (Shu et al. 2009; Levin et al. 2010). Furthermore, functional reorganization occurs with the occipital cortex in blind individuals involving auditory and tactile perception (Burton et al. 2004; Hötting and Röder 2009; Gagnon et al. 2010; Kupers et al. 2010; Collignon et al. 2011; Dormal et al. 2016), language processing (Amedi et al. 2004; Bedny et al. 2011; Striem-Amit et al. 2012; Watkins et al. 2012), braille reading (Sadato et al. 1996; Hamilton et al. 2000; Burton et al. 2002, 2012), and mathematics (Kanjlia et al. 2016).

Age has also been found to influence the alterations observed in the brains of blind individuals. The duration of blindness negatively correlates with WMV in the left pericalcarine and positively correlates with cortical thickness in the primary somatosensory cortex (Maller et al. 2016). The GMV in the primary sensory cortex and WMV in bilateral optic radiations in early blind individuals are associated with the age of blindness onset (Noppeney et al. 2005; Pan et al. 2007; Jiang et al. 2015). Cortical thickness is greater in individuals with early blindness than in those with late blindness and normal vision, while these latter two groups show no differences (Jiang et al. 2009).

Although previous studies have elegantly elucidated the pivotal plastic mechanisms of the occipital network in blind individuals, the longitudinal development of different profiles within the occipital network under congenital visual deprivation remains unknown. This knowledge gap arises from the use of a mixed subject sample of blindness in previous studies or the failure

Received: June 6, 2023. **Revised:** September 28, 2023. **Accepted:** September 29, 2023

to comprehensively examine network development, investigate both gray matter and white matter changes, or evaluate cognitive behaviors in the same study. To overcome these limitations, our study recruited 30 congenitally blind children and adults, along with 31 sighted controls. We examined gray matter regions and white matter connections within the occipital cortex as well as behaviors, revealing developmental differences between blind and sighted individuals (Fig. 1).

Materials and methods

Participants

Sixty-one Chinese participants were recruited for this study, and detailed demographic information is presented in Table 1. The participants consisted of 8 blind children, 22 blind adults, 10 sighted children, and 21 sighted adults. The blind and sighted control groups were carefully matched based on age [children: 10.63 ± 2.45 yr old vs. 10.80 ± 1.69 yr old, respectively; $t_{(16)} = 0.18$, $P = 0.86$; adults: 24.14 ± 5.31 yr old vs. 22.81 ± 2.58 yr old; $t_{(41)} = 1.03$, $P = 0.31$], sex [children: males/females = 6/2 vs. 7/3; $\chi^2_{(1)} = 0.06$, $P = 0.81$; adults: males/females = 7/15 vs. 10/11; $\chi^2_{(1)} = 1.12$, $P = 0.29$], and handedness (Oldfield 1971) [children: right/left handed = 7/1 vs. 10/0; $\chi^2_{(1)} = 1.32$, $P = 0.25$; adults: left/right handed = 21/1 vs. 21/0; $\chi^2_{(1)} = 0.98$, $P = 0.32$]. There were no significant group differences in the years of education obtained by the two groups of children [5.38 ± 2.39 vs. 5.50 ± 1.90; $t_{(16)} = 0.12$, $P = 0.90$]. However, blind adults had a significantly lower number of years of education than sighted adults [14.00 ± 2.27 vs. 16.38 ± 1.86; $t_{(41)} = 3.76$, $P < 0.001$]. This group difference in educational level may be attributed to the scarcity of special education schools in China, which resulted in fewer years of learning for blind adults.

All recruited blind individuals were congenitally blind and had acquired proficiency in using braille (blind children: 4.94 ± 2.27 yr of experience; blind adults: 13.95 ± 2.24 yr of experience). They self-reported never being able to distinguish colors, shapes, or motion. Among the 29 blind participants, 17 (blind children/blind adults: 4/13) self-reported that they had minimal light perception. The sighted participants had normal or corrected-to-normal vision. All participants were native Chinese speakers and reported no known neurological disorders, head injuries, or brain damage. They received compensation for their participation; adult participants and the parents or guardians of the child participants provided informed written consent. This study received full ethical approval from the Institutional Review Board of the National Key Laboratory of Cognitive Neuroscience and Learning, Beijing Normal University.

Behavioral data collection

Each participant underwent assessments of primary sensory perception and high-level cognitive processing abilities. Primary sensory perception was evaluated using a task specifically designed for this purpose, while high-level cognitive processing abilities were assessed using a word reading task. The word reading task was chosen for several reasons. First, word reading is a cognitive ability unique to humans and has been found to be associated with changes in the occipital cortex in blind individuals (Sadato et al. 1996; Bedny et al. 2011; Lin et al. 2022). Second, compared with other cognitive abilities (e.g. memory, attention) that develop from birth, word reading primarily develops from school age (Olulade et al. 2013). Therefore, word reading performance can be sensitive to developmental differences between children and adults in the present study. Third, word reading can be performed using different input modalities for the two visual abilities represented in the participant cohort: sighted individuals read visual written scripts, while blind individuals read tactile braille. Finally, word reading tasks can be flexibly designed to explore various processing cognitive components and neural pathways. In this study, we designed real word reading and nonword reading tasks that differed in several aspects, such as the involvement of semantic and phonological information (Vigneau et al. 2005; Bedny et al. 2011) and reliance on the ventral and dorsal pathways (Baron and Strawson 1976; Mandonnet and Duffau 2016).

The participants completed the tasks outside the scanner, with each conducted in a separate session using the DisplayMaster DirectX (DMDX) program (Forster and Forster 2003) on a PC for the sighted groups. For the blind groups, stimuli were presented on a braille display device (THDZ-40, http://www.qhqmx.com.cn/index.html). The order of stimulus presentation was pseudorandomized but consistent across all participants. Each participant performed the tasks in a quiet room and could request rest breaks as needed.

Real word reading

This task consisted of 40 items for the child groups and 88 items for the adult groups. Each item was either a single Chinese character (e.g. 跳 meaning jump, */tiao4/* with the pinyin indicating the tone of the preceding syllable) or a two-character Chinese word (e.g. 骆驼 meaning camel, */luo4tuo0/*). The words were presented visually on a screen or tactually on a braille display device. Participants were instructed to verbally report the word that they saw or touched as quickly as possible, and only the first complete response was scored for each item.

Nonword reading

Each nonword consisted of two Chinese characters (e.g. 致香, */zhi4xaing1/*) that together do not exist in the Chinese language corpus and have no meaning. There were 20 items for the child groups and 40 items for the adult groups. Participants were required to read the nonword stimuli aloud as quickly as possible, and only the first complete response was scored for each item.

Primary sensory perception

To assess primary perceptual processing, a perceptual task involving minimal semantic processing was used. For the sighted groups, the perceptual size-matching subtest from the Birmingham Object Recognition Battery ($n = 30$; Riddoch and Humphreys 1993) was employed. In each item, participants were asked to determine whether the size of two dots was the same and responded by pressing a button. This task was not suitable for the blind subjects because they needed to touch the objects successively rather than simultaneously, making it challenging to complete the task under this constraint and resulting in an inconsistent match in overall task difficulty between the two groups. Therefore, a different task was used for the blind group (i.e. meaningless symbol discrimination, $n = 18$) with a difficulty level comparable with that of the task for the sighted individuals. In each item, two meaningless symbols (e.g. "\" and "#") appeared in a row on the braille display device. Participants touched the symbols from left to right, determine if the two stimuli had the same shape, and responded by pressing a button.

Note that the word reading tasks for the child groups had fewer items than those for the adult groups. This was done to prevent children from becoming tired, bored, or uncooperative during testing. The number of items for the child groups were

Table 1. Demographic information of participants.

Subject group	Subject	Sex	Handedness	Years of age	Years of education	Cause of blindness	Light perception	Years of braille usage
Blind children								
	1	F	R	9	4	OND	Minimal	2.5
	2	F	R	11	6	ONH	Minimal	6
	3	M	L	13	7	ONH	None	7
	4	M	R	8	3	ROP	None	4
	5	M	R	8	3	ROP	None	3
	6	M	R	10	4	Microph-thalmia	None	3
	7	M	R	11	6	VH	Minimal	6
	8	M	R	15	10	ED	Minimal	9
Blind adults								
	1	F	R	19	13	RP	Minimal	13
	2	F	R	19	13	Unknown	Minimal	13
	3	F	L	19	12	Unknown	Minimal	12
	4	F	R	19	13	ONA	Minimal	13
	5	F	R	19	9	Unknown	Minimal	9
	6	F	R	20	14	ED	None	14
	7	F	R	21	9	MD	Minimal	9
	8	F	R	22	15	ONA	None	15
	9	F	R	22	15	Unknown	Minimal	15
	10	F	R	23	16	ROP	None	16
	11	F	R	25	12	Cataracts	None	12
	12	F	R	26	17	Unknown	None	17
	13	F	R	27	15	ONA	None	15
	14	F	R	29	12	ONA	Minimal	12
	15	F	R	35	15	Unknown	None	15
	16	M	R	20	14	ROP; ONA	None	14
	17	M	R	20	14	Unknown	Minimal	14
	18	M	R	25	16	Unknown	Minimal	16
	19	M	R	26	15	FD	Minimal	15
	20	M	R	26	18	Unknown	Minimal	18
	21	M	R	32	15	Cataracts	None	15
	22	M	R	37	16	Unknown	None	15
Sighted children								
	1	F	R	9	4	/	/	/
	2	F	R	10	4	/	/	/
	3	F	R	11	6	/	/	/
	4	M	R	9	4	/	/	/
	5	M	R	9	3	/	/	/
	6	M	R	11	5	/	/	/
	7	M	R	11	6	/	/	/
	8	M	R	11	6	/	/	/
	9	M	R	13	8	/	/	/
	10	M	R	14	9	/	/	/
Sighted adults								
	1	F	R	18	12	/	/	/
	2	F	R	20	14	/	/	/
	3	F	R	20	14	/	/	/
	4	F	R	20	14	/	/	/
	5	F	R	21	15	/	/	/
	6	F	R	21	15	/	/	/
	7	F	R	21	17	/	/	/
	8	F	R	24	17	/	/	/
	9	F	R	24	17	/	/	/
	10	F	R	26	18	/	/	/
	11	F	R	27	19	/	/	/
	12	M	R	22	16	/	/	/
	13	M	R	22	16	/	/	/
	14	M	R	23	16	/	/	/
	15	M	R	23	17	/	/	/
	16	M	R	23	17	/	/	/
	17	M	R	23	17	/	/	/
	18	M	R	23	17	/	/	/
	19	M	R	23	18	/	/	/
	20	M	R	27	19	/	/	/
	21	M	R	28	19	/	/	/

Note. ED = eyeball dysplasia; F = female; FD = fundus dysplasia; L = left-handed; M = male; MD = macular dysplasia; ONA = optic nerve atrophy; OND = optic nerve dysplasia; ONH = optic nerve hypoplasia; R = right-handed; ROP = retinopathy of prematurity; RP = retinitis pigmentosa; VH = vitreous hyperplasia.

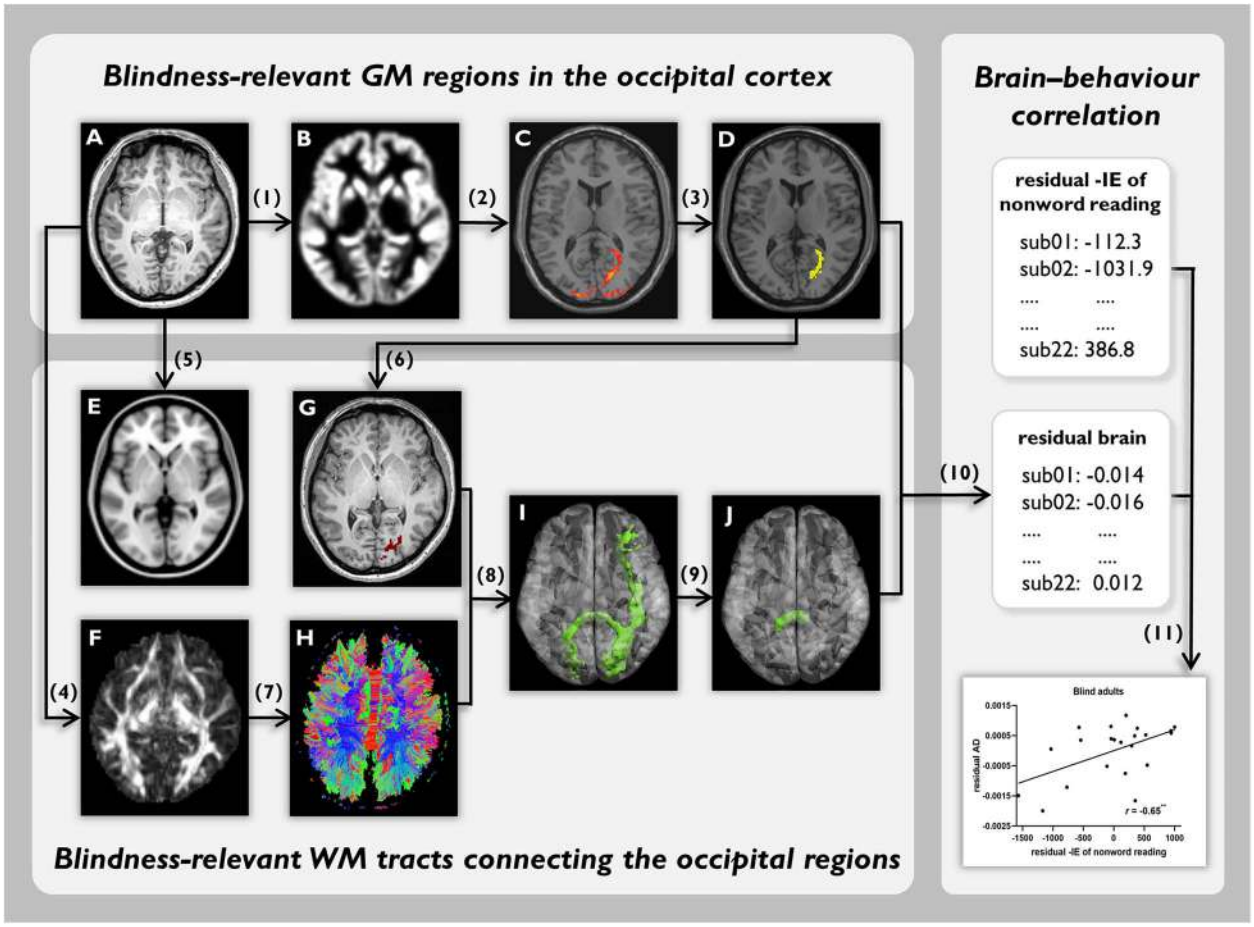

Fig. 1. Schematic flowchart for data analysis. (1) Generation of normalized, modulated, and smoothed GMV images (B) from native T1-weighted images (A) by VBM analysis. (2) Two-way ANCOVA for the GMV in the occipital cortex (AAL template: #43–#54) was conducted to identify ROIs (C) with a significant interactive effect. (3) A binary ROI mask was built in the MNI space for each ROI; the ROI mask of rCAL (D) is shown as an example. (4) Linear registration was performed to transform T1-weighted images (A) to native FA images (F), resulting in a linear transformation matrix (T) from the native T1 space to the native diffusion space. (5) Nonlinear registration from native T1-weighted images (A) to the T1 template of ICBM152 in MNI space was performed (E), resulting in a nonlinear transformation matrix (n-T) from native T1 space to MNI space. (6) Transformation of the ROI mask of rCAL in MNI space (D) to the native diffusion space was performed by applying the two inverse transformation matrices (T', and n-T') obtained from the previous two steps, resulting in a subject-specific ROI mask in the native diffusion space (G). (7) Reconstruction of all the WM fibers (H) in the whole brain from the native FA image (F) was performed by using DTI deterministic tractography. (8) Determination and normalization of the WM tract (I) passing through the ROI for each subject to the MNI space was conducted. (9) A separate two-way ANCOVA was performed for each measure (i.e. FA, AD, MD, and RD) of the WM tract and used to identify the WM clusters with significant interactive effects; the WM cluster in the lFM from the difference analysis of AD is shown as an example (J) demonstrating a significant interactive effect. (10) Extraction of the residual values of brain indicators (i.e. the mean residual GMV value in each ROI and the sum of the residual WM measures' value in each significant WM cluster) was conducted for each subject in each group after controlling for sex and TIV, taking the residual AD of the lFM in blind adults as an example. (11) Pearson correlation analysis was conducted between the residual values of brain indicators and the performance of each behavior task (primary sensory perception task: -IE value; real word reading task & nonword reading task: Residual -IE value, controlling for the -IE of the primary sensory perception task), taking the residual AD of the lFM and nonword reading task in blind adults as an example. AAL = Automated Anatomical Labeling; AD = axial diffusivity; ANCOVA = analysis of covariance; FA = fractional anisotropy; GM = gray matter; GMV = gray matter volume; lFM = left forceps major; MNI = Montreal Neurological Institute; MD = mean diffusivity; rCAL = right calcarine fissure; RD = radial diffusivity; ROI = region of interest; TIV = total intracranial volume; VBM = voxel-based morphometry; WM = white matter; -IE = negated inverse efficiency.

determined according to previous studies investigating children's reading abilities (e.g. Hu and Catts 1998; Greenberg et al. 2002; Griffiths and Snowling 2002; Goswami et al. 2003; Dillon and Pisoni 2004). Importantly, the items for the child groups were randomly selected from the pool of items used for adults.

MRI data acquisition

All MRI scans were conducted on the same 3 T Siemens Prisma scanner at the Imaging Center for Brain Research, Peking University. Two types of images were collected, as described below.

T1-weighted images

Sagittal acquisition was performed using a magnetization-prepared rapid gradient-echo (MP-RAGE) sequence with the following imaging parameters: 192 sagittal slices covering the entire brain; echo time (TE), 2.98 ms; repetition time (TR), 2530 ms; inversion time (TI), 1100 ms; 1-mm slice thickness; voxel size, $0.5 \times 0.5 \times 1.0$ mm^3; flip angle, 7°; and field of view (FOV), 256×256 mm^3.

Diffusion-weighted imaging

Axial acquisition was performed using a single-shot echo-planar imaging (EPI) sequence. The integral parallel acquisition technique (iPAT) with an acceleration factor of 2 was used; this allowed reduction of the acquisition time and image distortion from susceptibility artifacts. The parameters were as follows: 70 axial slices covering the whole brain; TE, 73 ms; TR,

5100 ms; diffusion directions, 30; b-value 1, 0 s/mm^2; b-value 2, 1000 s/mm^2; b-value 3, 2000 s/mm^2; 2-mm slice thickness; voxel size, 2.0 × 2.0 × 2.0 mm^3; flip angle, 60°; and FOV, 224 × 224 mm^2.

Behavioral data preprocessing

The accuracy and reaction time (RT) of each item were recorded for analysis. To mitigate the influence of extreme subject responses, we excluded any item with a difference between its RT and the average RT of all items that was greater than twice the standard deviation of the RTs for each participant in each task. In addition, we employed the negated inverse efficiency (-IE) measure to account for potential trade-off effects between speed and accuracy. The inverse efficiency was computed as the ratio of the average RT of correct items to the overall accuracy of all items ((Townsend and Ashby 1983). The sign of the inverse efficiency was reversed to ensure that a higher -IE value for a subject in a particular task corresponded to better performance in that task.

MRI data preprocessing

T1-weighted images

These images were analyzed using Statistical Parametric Mapping version 12 (SPM12) (http://www.fil.ion.ucl.ac.uk/spm/software/spm12/) with default parameters incorporating the Diffeomorphic Anatomical Registration Through Exponentiated Lie Algebra (DARTEL) algorithm (Ashburner 2007). The image processing procedure comprised (i) tissue segmentation using the DARTEL algorithm and (ii) spatial normalization to Montreal Neurological Institute (MNI) standard space; (iii) modulation by the Jacobian determinants generated during spatial normalization (Goldszal et al. 1998; Ashburner and Friston 2000), with a voxel size of 1.5 × 1.5 × 1.5 mm^3 after image normalization and modulation; and (iv) image smoothing with a Gaussian kernel of 4 mm full-width at half maximum (Fig. 1). Considering that the shape and size of children's brains are different from those of adults, we used the age-specific Chinese pediatric atlas (CHN-PD) (Zhao et al. 2019) (https://www.nitrc.org/projects/chn-pd) for normalization in the voxel-based morphometry (VBM) analysis for child participants to improve the normalization accuracy. To compare the brain structural differences between children and adults in the following analyses, we transformed the children's images into the same MNI space as the adults' images (Zhao et al. 2019; Lin et al. 2022; Xia et al. 2022). Then, two-way analysis of covariance (ANCOVA) of the GMV in the occipital cortex was conducted among the four groups, and the reported gray matter clusters with significant interactive effects were defined as regions of interest (ROIs) for the subsequent analyses. The procedures are described in detail as follows.

Diffusion-weighted images

These images were preprocessed using a pipeline tool for analyzing brain diffusion images, PANDA (Cui et al. 2013) (http://www.nitrc.org/projects/panda/). The procedure included the following steps: (i) converting the raw diffusion files into a single 4D image; (ii) extracting brain tissue from the diffusion-weighted image, skull removal, and cropping gap; (iii) producing the images from which diffusion metrics [i.e. FA, axial diffusivity (AD), MD, and RD)] could be extracted; (iv) normalizing the diffusion metric images of native space to MNI space with a voxel size of 2.0 × 2.0 × 2.0 mm^3; and (v) smoothing the images with a 6 mm Gaussian kernel.

To determine the white matter tracts that passed through the ROIs defined in the gray matter analyses, we performed deterministic fiber tracking with Diffusion Toolkit (http://trackvis.org/dtk/) (Wang et al. 2007) in the individual native diffusion space. For each ROI in each individual, the ROI mask in MNI space obtained from the previous gray matter statistical analysis was initially transformed into the native diffusion space. The detailed procedure included the following steps (Fig. 1). (i) Briefly, the individual T1-weighted image was coregistered to the individual FA image in the native diffusion space via linear transformation. (ii) A nonlinear registration from the native T1-weighted image to the T1 template of ICBM152 in MNI space was conducted. (iii) The ROI mask in MNI space was transformed to the native diffusion space by applying the two resulting inverse transformations obtained above, which resulted in a subject-specific ROI mask in the native diffusion space. (iv) Then, deterministic fiber tracking was conducted to reconstruct all the white matter fibers in the whole brain by utilizing the fiber assignment by continuous tracking (FACT) algorithm (Mori et al. 1999; Mori and van Zijl 2002). Tracking was terminated if/when the crossing angle of two consecutive orientations was >45° or the FA value was <0.2. (v) We then extracted the white matter fibers passing through or terminating in the ROI. Finally, the tract images were transformed into MNI space for subsequent statistical analysis.

Statistical analyses

Behavioral performance

Two-way analysis of variance (ANOVA) with two levels for vision (blind vs. sighted) * two levels for age (children vs. adults) was performed with the -IE measures from each task. The two-tailed independent two-sample *t* test was used for post hoc analysis. All comparisons were corrected by false discovery rate (*FDR*) ($q < 0.05$).

Blindness-relevant gray matter regions in the occipital cortex

To identify the blindness-relevant gray matter regions in the occipital cortex, we conducted two-way ANCOVA with two levels for vision (blind vs. sighted) * two levels for age (children vs. adults) on the basis of VBM for the GMV values in the occipital cortex. In this analysis, the two covariates of no interest were sex and total intracranial volume (TIV) (Pell et al. 2008; Barnes et al. 2010; Peelle et al. 2012). TIV was calculated as the sum of the normalized, modulated, smoothed tissue segments (gray matter + white matter + cerebrospinal fluid). We treated the occipital regions (#43–#54) in the Automated Anatomical Labeling (AAL) template (Tzourio-Mazoyer et al. 2002) as the gray matter mask. The clusters with significant interactions (*FDR* corrected, $q < 0.001$; cluster size > 150 voxels) were defined as ROIs for the subsequent analyses (Fig. 1). To further reveal the pattern of the interaction in each ROI, post hoc two-tailed two-sample *t* tests were performed to compare the mean GMV values among the four subject groups (*FDR* corrected, $q < 0.05$).

Blindness-relevant white matter tracts connecting with the occipital regions

To identify white matter tracts that were influenced by blindness and connected with the aforementioned occipital ROIs, we conducted two-way ANCOVA. This analysis involved two levels for vision (blind vs. sighted) * two levels for age (children vs. adults), with sex and TIV considered as additional covariates for each white matter measure (including FA, AD, MD, and RD) of the white matter tract connecting each ROI. Gaussian random field (*GRF*) correction (voxel-level $P < 0.005$, cluster-level $P < 0.05$; cluster size > 15 voxels) was utilized with a white matter mask for the white matter tract connecting each ROI, created by the sum

Table 2. Mean (standard deviation) values for the three behavioral tasks for each subject group.

	Task	Blind children	Blind adults	Sighted children	Sighted adults
ACC	Real word reading	0.87 (0.17)	0.93 (0.05)	0.97 (0.03)	0.99 (0.01)
	Nonword reading	0.80 (0.18)	0.98 (0.03)	0.93 (0.05)	0.97 (0.03)
	Primary sensory perception	0.89 (0.09)	0.94 (0.08)	0.83 (0.07)	0.87 (0.06)
RT (ms)	Real word reading	2367.21 (706.28)	2014.92 (462.11)	729.09 (115.07)	823.24 (175.61)
	Nonword reading	2552.33 (1088.42)	2513.48 (667.08)	1006.43 (220.11)	938.71 (221.14)
	Primary sensory perception	3848.58 (1590.17)	2583.25 (674.34)	964.06 (288.64)	833.74 (213.60)
-IE	Real word reading	−2962.39 (1653.78)	−2077.05 (476.55)	−755.43 (121.82)	−835.34 (184.60)
	Nonword reading	−3910.54 (3623.78)	−2724.06 (776.02)	−1080.09 (233.65)	−965.91 (233.52)
	Primary sensory perception	−4483.34 (2316.21)	−2752.19 (695.53)	−1174.99 (390.92)	−949.92 (211.16)

Note. ACC = accuracy; RT = reaction time; -IE = negated inverse efficiency.

of voxels containing white matter fibers for each group (Fig. 1). Within each group, the voxels were considered to contain fibers if no <20% of subjects had fibers in them. Then, we adopted the John Hopkins University (JHU) International Consortium for Brain Mapping atlas (Hua et al. 2008), a widely used human brain white matter tractography template, to identify the white matter tracts with significant differences between groups. Post hoc two-tailed two-sample *t* tests were performed (*FDR* corrected, $q < 0.05$).

Behaviors associated with the blindness-relevant occipital structural network

To elucidate the changes in cognitive function accompanied by structural alterations in blind individuals, we examined the relationship between brain structure (gray matter cortex, white matter connectivity) alterations and cognitive behavioral performance. Specifically, we performed Pearson correlation analysis between (i) the mean residual GMV values of the ROIs and (ii) the sum of the residual FA, AD, MD, RD values for significant white matter tracts (after controlling for sex and TIV) and the performance of three behavior tasks [primary sensory perception task: -IE value; real word reading task and nonword reading task: residual -IE value (controlling for the -IE value of the primary sensory perception task, to control the influence of different input modalities in two reading tasks between the blind and the sighted)] across subjects within each group (*FDR* corrected, $q < 0.05$) (Fig. 1).

Note that all blind subjects were congenital blind, who experienced vision loss from birth. The age of blindness onset was uniformly zero years, resulting in no variance within this cohort. Therefore, we did not consider it in the statistical analyses.

Results

Behavioral performance

Table 2 shows the mean accuracy, RTs, and -IE values for each task in each subject group. For the -IE in each task, we separately conducted two-way ANOVA with two levels for vision (blind vs. sighted) * two levels for age (children vs. adults). There were significant interactions of age and vision for -IE in the real word reading [$F_{(1, 57)} = 6.75$, $P = 0.01$] and primary sensory perception [$F_{(1, 57)} = 8.13$, $P = 0.006$] tasks, while the interaction term was not significant in the nonword reading task [$F_{(1, 57)} = 0.10$, $P = 0.17$]. Between the two blind groups, the adults performed better than the children in both real word reading [$t_{(28)} = 2.32$, *FDR* corrected $P = 0.04$] and primary sensory perception [$t_{(28)} = 3.21$, *FDR* corrected $P = 0.004$]. In contrast, for the two sighted groups, the adults performed comparably with the children in both tasks [real word reading: $t_{(29)} = 1.24$, *FDR* corrected $P = 0.22$; primary sensory perception: $t_{(29)} = 2.10$, *FDR* corrected $P = 0.05$].

Blindness-relevant gray matter regions in the occipital cortex

Using two-way ANCOVA (covarying for sex and TIV) for the voxelwise GMV values in the occipital mask, we obtained five ROIs with significant interaction (*FDR* corrected, $q < 0.001$; cluster size > 150 voxels) (Fig. 2). The ROIs included the left calcarine fissure [lCAL; peak coordinates: $x = -9$, $y = -100.5$, $z = -13.5$; $F_{(1,57)} = 40.72$; 181 voxels], left superior occipital gyrus [lSOG; peak coordinates: $x = -16.5$, $y = -97.5$, $z = 12$; $F_{(1,57)} = 85.18$; 1688 voxels], right CAL [rCAL; peak coordinates: $x = 18$, $y = -75$, $z = 13.5$; $F_{(1,57)} = 153.24$; 614 voxels], right LING [rLING; peak coordinates: $x = 27$, $y = -91.5$, $z = -13.5$; $F_{(1,57)} = 87.75$; 1031 voxels], and right middle occipital gyrus [rMOG; peak coordinates: $x = 42$, $y = -90$, $z = 1.5$; $F_{(1,57)} = 67.73$; 595 voxels].

The interaction of the GMV values of the five ROIs demonstrated two different patterns (Fig. 2). The first pattern was present in the three anterior ROIs (i.e. lSOG, rCAL, and rLING). Regarding the two groups of children, the GMV values in the blind group were significantly lower than those in the sighted group [lSOG: $t_{(16)} = 8.75$; rCAL: $t_{(16)} = 8.89$; rLING: $t_{(16)} = 7.37$; *FDR* corrected $Ps < 0.001$]. Regarding the two groups of adults, compared with the sighted group, the blind group had significantly higher GMV values [lSOG: $t_{(41)} = 5.47$, *FDR* corrected $P = 0.02$; rCAL: $t_{(41)} = 2.49$, *FDR* corrected $P < 0.001$; rLING: $t_{(41)} = 5.79$, *FDR* corrected $P < 0.001$]. Regarding the two sighted groups, the GMV values of the children were significantly higher than those of the adults [lSOG: $t_{(29)} = 12.48$; rCAL: $t_{(29)} = 15.83$; rLING: $t_{(29)} = 11.50$; *FDR* corrected $Ps < 0.001$]. Regarding the two blind groups, compared with the adults, the children had significantly lower GMV values in the rLING [$t_{(28)} = 2.33$, *FDR* corrected $P = 0.03$]. Compared with those of sighted individuals, the GMV values of these three anterior ROIs in blind individuals were decreased in childhood but increased in adulthood. From childhood to adulthood, the GMV values of these three anterior ROIs decreased in sighted individuals but increased or were stable in the blind individuals.

The second pattern was evident in the two posterior ROIs (lCAL and rMOG). Regarding the two groups of children, the GMV values in the blind group were significantly higher than those in the sighted group [lCAL: $t_{(16)} = 4.55$, *FDR* corrected $P < 0.001$; rMOG: $t_{(16)} = 3.07$, *FDR* corrected $P = 0.01$]. Regarding the two groups of adults, compared with the sighted group, the blind group had significantly lower GMV values [lCAL: $t_{(41)} = 4.95$; rMOG: $t_{(41)} = 7.37$; *FDR* corrected $Ps < 0.001$]. Regarding the two sighted groups, the GMV values in adults were significantly higher than those in children [lCAL: $t_{(29)} = 9.18$; rMOG: $t_{(29)} = 10.95$; *FDR* corrected

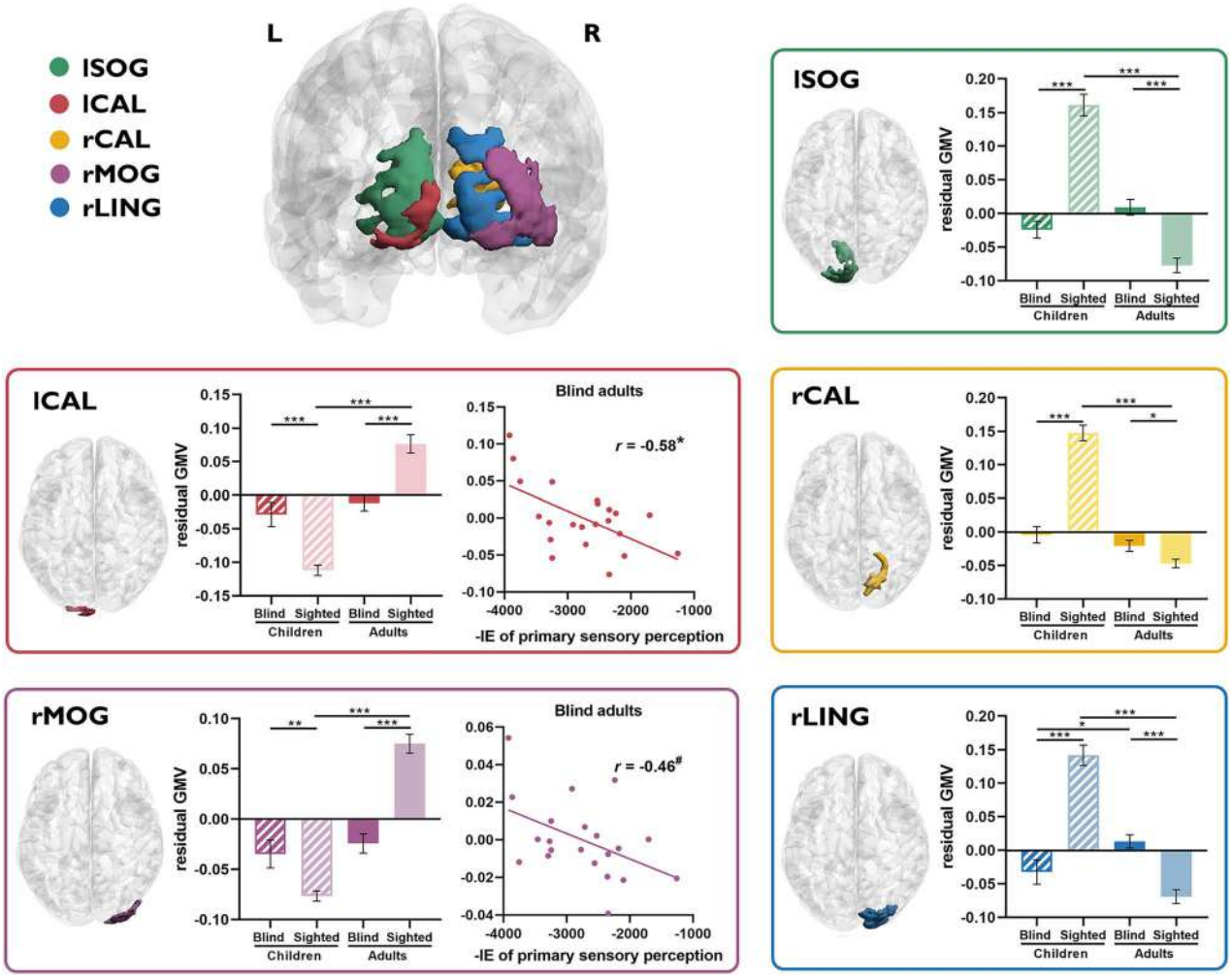

Fig. 2. Occipital gray matter regions with significant interactions (vision * age) for the GMV values and their associated behaviors. The five regions with significant interactions and their results are shown in different colors. Error bars indicate the standard error of the mean. *FDR* corrected ($q < 0.05$): #$P < 0.15$; *$P < 0.05$; **$P < 0.01$; ***$P < 0.001$. CAL = calcarine fissure; GMV = gray matter volume; l/L = left hemisphere; LING = lingual gyrus; MOG = middle occipital gyrus; r/R = right hemisphere; SOG = superior occipital gyrus; -IE = negated inverse efficiency.

Ps < 0.001]. However, the values were not significantly different between the two blind groups in the two ROIs [lCAL: $t_{(28)} = 0.76$; rMOG: $t_{(28)} = 0.58$; *FDR* corrected *Ps* > 0.46]. The GMV values of the two posterior ROIs in blind individuals increased in childhood but decreased in adulthood compared with those in sighted individuals. From childhood to adulthood, the GMV values of the two posterior ROIs increased in sighted individuals but remained unchanged in blind individuals.

Behaviors associated with blindness-relevant occipital regions

We assessed the correlations of the mean residual GMV value of each of the five ROIs with performance of three behavioral tasks across subjects in each group. Significant or marginally significant correlations were observed only in the blind adult group (Table 3 and Fig. 2). The following correlations with mean residual GMV were negative: the lCAL-primary sensory perception correlation ($r = -0.58$, *FDR* corrected $P = 0.02$) and the rMOG-primary sensory perception correlation ($r = -0.46$, $P = 0.03$, *FDR* corrected $P = 0.08$). These results suggest that long-term congenital blindness is correlated with plastic reorganization of the posterior occipital cortices, enabling their involvement in processing tactile perception in adulthood.

Blindness-relevant white matter tracts connecting with the occipital regions

For each of the five identified ROIs, we first obtained a mask including all the white matter fibers connected with that ROI. In the mask, we performed two-way ANCOVA (partialling out sex and TIV) for each white matter measure (FA, AD, MD, and RD) and masked the clusters with significant interaction effects (*GRF* corrected, voxel-level $P < 0.005$, cluster-level $P < 0.05$; cluster size > 15 voxels). We found that the only significant interaction appeared in the white matter mask connecting with the rCAL. Moreover, the effects were similar across the four measures, including the peak locations and the cluster sizes. The significant clusters were distributed among three tracts on the JHU template: right IFOF (rIFOF), left forceps major (lFM), and right FM (rFM) (Table 4 and Fig. 3).

The patterns of interaction effects were similar across the tracts (Fig. 3). Regarding the two groups of children, the white matter measure values in the blind group were significantly lower than those in the sighted group [rIFOF: $t_{(16)} > 2.74$, *GRF* corrected *Ps* < 0.02; lFM: $t_{(16)} > 10.25$, *GRF* corrected *Ps* < 0.001; rFM: $t_{(16)} > 3.90$, *GRF* corrected *Ps* < 0.001]. Regarding the two groups of adults, compared with those of the sighted group, the white matter measures values of the blind group were significantly reduced

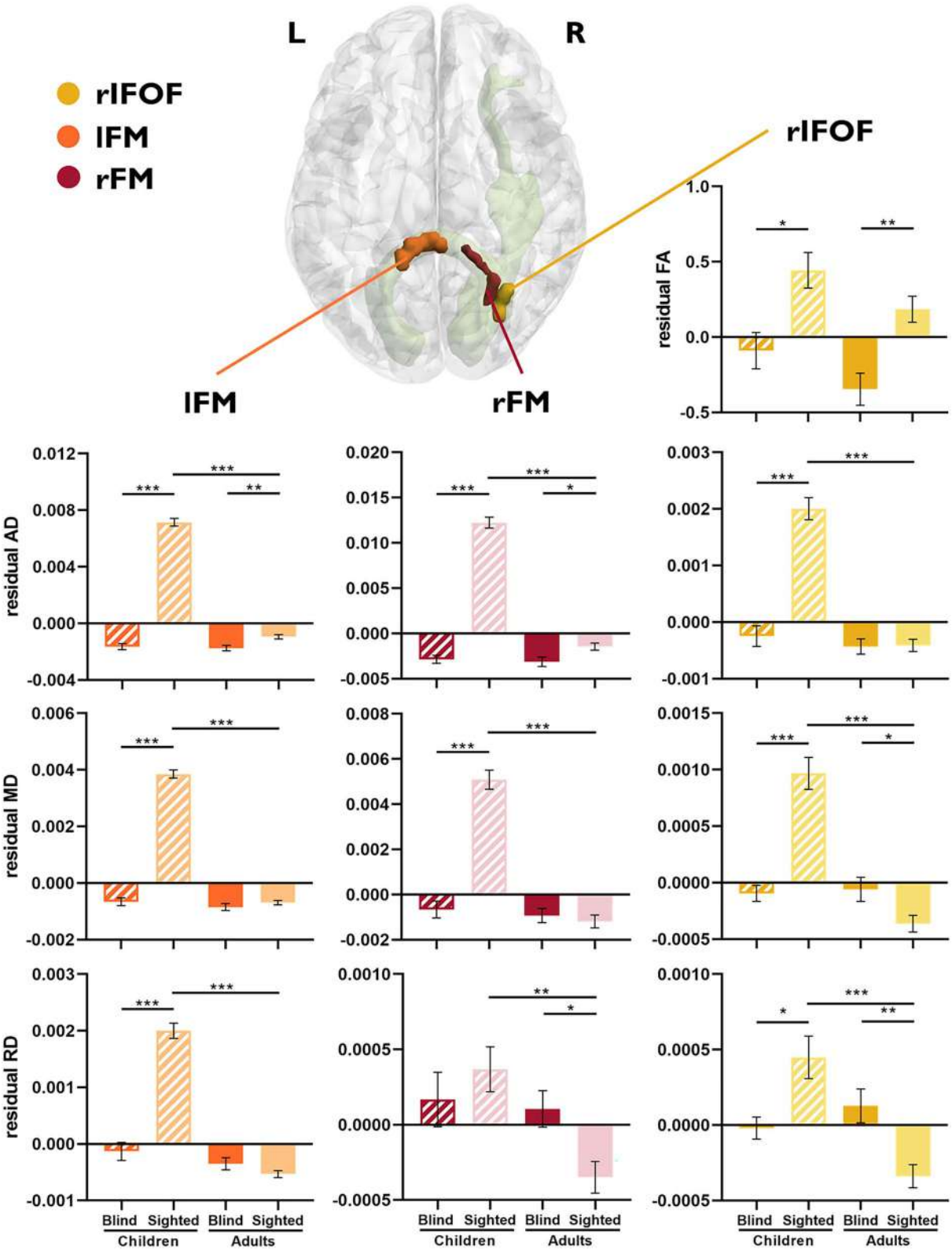

Fig. 3. Occipital white matter tracts with significant interactions (vision * age). The white matter fibers passing through the rCAL are shown in green. Three clusters with significant interactions and their results are shown in different warm colors. Error bars indicate the standard error of the mean. *FDR* corrected ($q < 0.05$): *$P < 0.05$; **$P < 0.01$; ***$P < 0.001$. AD = axial diffusivity; CAL = calcarine fissure; FA = fractional anisotropy; FM = forceps major; IFOF = inferior fronto-occipital fasciculus; l/L = left hemisphere; MD = mean diffusivity; r/R = right hemisphere; RD = radial diffusivity.

Table 3. Correlation coefficients between the residuals of the GMV (controlling for sex and TIV) and the performance of three tasks (-IE of primary sensory perception task; and residual -IE of two reading tasks, after controlling for the -IE of primary sensory perception task) in each ROI for each subject group.

Subject group	Task	ROI				
		lCAL	lSOG	rCAL	rLING	rMOG
Blind children						
	Real word reading	0.10	−0.57	−0.18	0.16	−0.09
	Nonword reading	−0.20	−0.56	0.05	0.43	0.06
	Primary sensory perception	0.47	0.60	0.21	0.21	0.56
Blind adults						
	Real word reading	−0.24	−0.26	−0.24	−0.01	0.08
	Nonword reading	−0.40	−0.24	−0.19	0.04	−0.18
	Primary sensory perception	−0.58*	−0.25	0.18	−0.28	−0.46#
Sighted children						
	Real word reading	0.47	0.05	−0.55	0.22	0.54
	Nonword reading	0.42	0.05	−0.63	0.11	0.48
	Primary sensory perception	0.40	0.22	−0.17	0.25	0.63
Sighted adults						
	Real word reading	−0.11	−0.09	0.16	0.06	−0.02
	Nonword reading	−0.28	−0.23	0.15	0.02	−0.02
	Primary sensory perception	−0.21	−0.16	0.24	−0.16	−0.33

Note. *FDR* corrected ($q < 0.05$): #$P < 0.15$; *$P < 0.05$. CAL = calcarine fissure; GMV = gray matter volume; l = left hemisphere; LING = lingual gyrus; MOG = middle occipital gyrus; r = right hemisphere; ROI = region of interest; SOG = superior occipital gyrus; TIV = total intracranial volume; -IE = negated inverse efficiency.

Table 4. White matter tracts with significant interactions in ANCOVA for each white matter measure.

White matter tract	White matter measures	x	y	z	Cluster size	F value
rIFOF	FA	30	−72	0	16	16.81
	AD	30	−72	0	16	20.39
	MD	30	−72	0	16	21.92
	RD	30	−72	0	16	23.45
lFM	AD	0	−38	8	27	35.58
	MD	0	−38	8	28	37.54
	RD	2	−38	8	27	39.46
rFM	AD	20	−46	12	67	155.61
	MD	20	−46	12	60	119.11
	RD	28	−60	16	17	18.43

Note. AD = axial diffusivity; ANCOVA = analysis of covariance; FA = fractional anisotropy; MD = mean diffusivity; RD = radial diffusivity.

or unchanged in the bilateral FM [lFM: $t_{(41)} = 3.18$, *GRF* corrected $P = 0.004$; rFM: $t_{(41)} > 2.56$, *GRF* corrected $Ps < 0.02$] and showed a more complex reorganization pattern in the rIFOF [$t_{(41)} > 2.33$, *GRF* corrected $Ps < 0.03$]. Regarding the two sighted groups, the white matter measures values were significantly lower in the adults than in the children [rIFOF: $t_{(29)} > 5.35$, *GRF* corrected $Ps < 0.001$; lFM: $t_{(29)} > 19.68$, *GRF* corrected $Ps < 0.001$; rFM: $t_{(29)} > 3.90$, *GRF* corrected $Ps < 0.002$]. Regarding the two blind groups, the differences in the measures did not reach the significance level (*GRF* corrected, $Ps > 0.05$). These results indicate that the white matter values of these tracts were lower in blind individuals than in sighted individuals in both childhood and adulthood, but the differences in adulthood were reduced to no difference from those in childhood. From childhood to adulthood, the white matter values of these tracts decreased in sighted individuals but were unchanged in blind individuals.

Behaviors associated with blindness-relevant occipital tracts

We assessed the correlations of the mean residual of each white matter measure in each of the three white matter clusters (rIFOF, lFM, and rFM) with the performance of three behavioral tasks across subjects in each group. Significant correlations with -IE only appeared in the lFM and rFM in blind adults (Table 5 and Fig. 4). Significant positive correlations in the lFM appeared for each pair between one of the three white matter measures (AD, MD, and RD) and one of the two reading tasks ($rs > 0.49$, *FDR* corrected $Ps < 0.03$). Each of the three white matter measures (AD, MD, and RD) of the rFM was significantly or marginally significantly positively correlated with the nonword reading task (AD: $r = 0.47$, $P = 0.03$, *FDR* corrected $P = 0.12$; MD: $r = 0.57$, *FDR* corrected $P = 0.05$; RD: $r = 0.43$, $P = 0.05$, *FDR* corrected $P = 0.14$). These results show that long-term congenital blindness leads to a correlation between the bilateral FM tracts and braille reading in adulthood.

Discussion

By recruiting congenitally blind participants across different age groups (children and adults) as well as sighted controls, we investigated the developmental reorganization of gray and white matter in the occipital cortex, as well as behavioral changes resulting from visual experience deprivation. Our findings revealed distinct developmental patterns in the anterior and posterior occipital regions (lSOG, rCAL, rLING, lCAL, and rMOG) when comparing the GMV values of blind individuals with those of sighted individuals. Specifically, the GMV values of blind individuals decreased in childhood and increased in adulthood in the anterior occipital

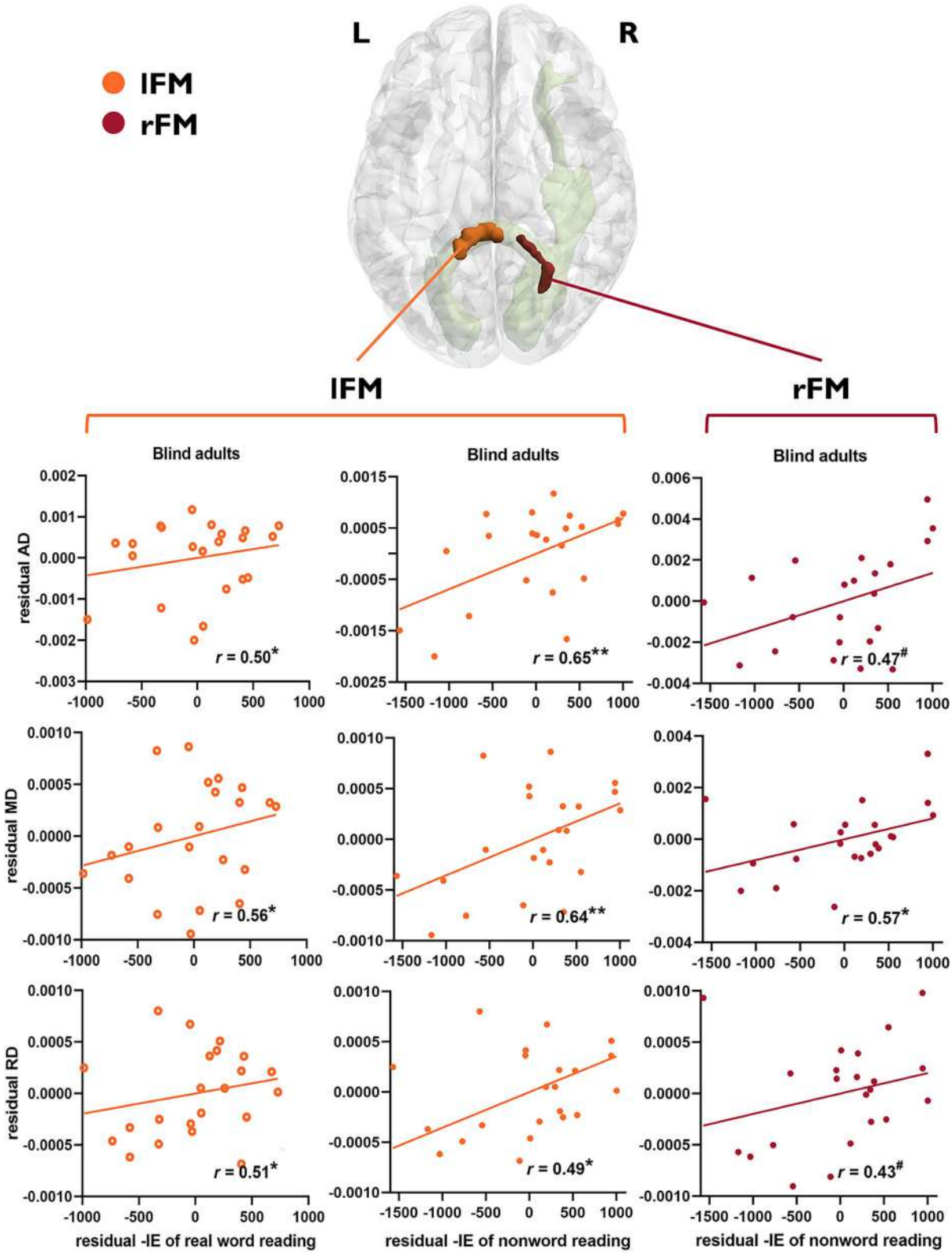

Fig. 4. Significant brain-behavior correlations in the occipital white matter tracts with significant interactions (vision * age). The white matter fibers passing through the rCAL are shown in green. The two white matter clusters with significant correlations and their results are shown in different warm colors. *FDR* corrected ($q < 0.05$): #P < 0.15; *P < 0.05; **P < 0.01. AD = axial diffusivity; CAL = calcarine fissure; FM = forceps major; l/L = left hemisphere; MD = mean diffusivity; r/R = right hemisphere; RD = radial diffusivity; -IE = negated inverse efficiency.

Table 5. Correlation coefficients between the residuals of the white matter measures (controlling for sex and TIV) and the performance of three tasks (-IE of primary sensory perception task; and residual -IE of two reading tasks, after controlling for the -IE of primary sensory perception task) in each tract within each group.

Subject group	Task	rIFOF				lFM			rFM		
		FA	AD	MD	RD	AD	MD	RD	AD	MD	RD
Blind children											
	Real word reading	−0.56	−0.07	0.36	0.64	0.52	0.40	0.04	0.70	0.35	0.12
	Nonword reading	−0.41	0.00	0.35	0.56	0.15	0.16	0.07	0.43	0.17	0.02
	Primary sensory perception	−0.30	−0.48	−0.30	0.04	−0.28	−0.59	−0.55	0.01	−0.41	−0.46
Blind adults											
	Real word reading	0.01	0.29	0.21	0.14	0.50*	0.56*	0.51*	0.24	0.36	0.25
	Nonword reading	−0.13	0.40	0.38	0.30	0.65**	0.64**	0.49*	0.47#	0.57*	0.43#
	Primary sensory perception	−0.10	0.25	0.28	0.25	0.17	0.23	0.26	0.11	0.19	0.13
Sighted children											
	Real word reading	0.35	−0.01	−0.24	−0.35	−0.24	−0.30	−0.24	0.33	−0.13	−0.27
	Nonword reading	0.45	−0.10	−0.37	−0.48	−0.19	−0.30	−0.29	0.23	−0.22	−0.32
	Primary sensory perception	0.59	0.58	0.17	−0.14	−0.14	−0.05	−0.19	0.09	−0.14	−0.17
Sighted adults											
	Real word reading	−0.36	−0.01	0.25	0.37	−0.32	−0.23	0.06	0.16	0.26	0.20
	Nonword reading	−0.44	−0.05	0.25	0.41	−0.15	−0.04	0.18	0.23	0.41	0.35
	Primary sensory perception	−0.12	−0.41	−0.33	−0.16	−0.15	−0.12	0.02	−0.35	−0.18	0.00

Note. FDR corrected ($q < 0.05$): $^{\#}P < 0.15$; $^{*}P < 0.05$; $^{**}P < 0.01$. AD = axial diffusivity; FA = fractional anisotropy; FM = forceps major; IFOF = inferior fronto-occipital fasciculus; l = left hemisphere; MD = mean diffusivity; r = right hemisphere; RD = radial diffusivity; TIV = total intracranial volume; -IE = negated inverse efficiency.

regions (lSOG, rCAL, and rLING), while the opposite developmental pattern was observed in the posterior occipital regions (lCAL and rMOG). With increasing age, we observed that the GMV values of sighted individuals decreased in anterior occipital regions and increased in posterior occipital regions. In contrast, the GMV values in the blind individuals remained unchanged or exhibited the inverse developmental trajectory. This suggests that long-term congenital blindness leads to plastic reorganization in the occipital cortex, enabling the posterior regions to respond to tactile stimuli and contribute to adult blind individuals.

Furthermore, we examined white matter measures in three specific white matter tracts (rIFOF, lFM, and rFM) connected to the rCAL in blind individuals. Compared with sighted individuals, blind individuals demonstrated a decrease in these measures during childhood, with the differences diminishing or even disappearing in adulthood. In addition, with age, these values decreased in sighted individuals but were unchanged in blind individuals. Interestingly, long-term visual loss resulted in the bilateral FM tracts participating in braille reading during blind adulthood.

Overall, our study provides valuable insights into the developmental plasticity of different occipital cortex profiles following congenital visual loss.

Morphological alterations in the occipital cortex

In sighted individuals, the occipital lobe serves as the primary visual processing center in the brain and encompasses various anatomical regions of the visual cortex. Previous research has established that gray matter morphology in the occipital cortex can undergo plastic changes in response to visual loss (Ptito et al. 2008; Bridge et al. 2009; Jiang et al. 2009, 2015; Park et al. 2009; Voss and Zatorre 2012; Yang et al. 2014; Li et al. 2017). However, these studies primarily focused on examining the effects of visual deprivation at a specific developmental stage, either during childhood or adulthood. Consequently, it has been challenging to determine the longitudinal developmental trajectories of gray matter alterations resulting from long-term visual deficits. To address this gap, the present study recruited two samples of congenitally blind individuals spanning different age groups (children and adults) as well as two control groups of sighted individuals. Our findings revealed distinctive developmental trajectories in gray matter morphology within five occipital regions.

Regarding the three anterior occipital regions (lSOG, rCAL, and rLING), the reduced GMV observed in congenitally blind individuals during childhood may be attributed to structural atrophy associated with the loss of visual function (Ptito et al. 2008; Bridge et al. 2009; Jiang et al. 2015). The axons and synapses pruned during development are typically experience-dependent phenomena in normally sighted individuals (Kolb and Whishaw 1998). In adulthood, the increased GMV in blind adults might indicate that these three regions were not recruited by cognitive functions and lacked experience-dependent cortical pruning. From childhood to adulthood, the reduction in GMV in the sighted individuals might also be due to cognitive functional specialization, which results in experience-dependent cortical pruning of neurons unrelated to current cognitive function. However, for congenitally blind individuals, the unchanged GMV values in these regions might be because the regions are "idle" after visual loss and not recruited by new cognitive demands, suggesting that the neurons in these regions were not pruned. This is consistent with our results indicating that these three regions were not correlated with the performance of tactile perception and braille reading tasks in either blind group (Fig. 2).

Regarding the two posterior occipital regions (lCAL and rMOG), our findings indicated an increase in the GMV in childhood followed by a reduction in adulthood among blind individuals. In adulthood, the reduction in the GMV in blind individuals may be attributed to cognitive functional specialization, a phenomenon typically observed in normally sighted individuals. This specialization leads to experience-dependent cortical pruning of neurons unrelated to the current cognitive function (Bridge et al. 2009; Jiang et al. 2009; Raznahan et al. 2011; Anurova et al. 2015). The cognitive functionality of these regions in blind individuals is influenced by cross-modal plasticity, enabling them to assume new tactile cognitive functions. With increasing age, the GMV values in sighted individuals increased, which may be interpreted as evidence of neuronal development after birth (Giedd et al. 1999;

Gogtay et al. 2004; Lenroot et al. 2007; Groeschel et al. 2010; Raznahan et al. 2011; Mills et al. 2016). However, the GMV values in congenially blind individuals were unchanged with age. This may be because the cognitive functionality of these regions in blind individuals was affected by cross-modal plasticity, taking on new tactile cognitive functions. Indeed, our results showed the structural values of these regions were correlated with the performance of the primary tactile perception.

Reorganization of white matter connections from the occipital cortex

Brain plasticity involves structural reorganization, which may be attributed to increased myelination of intracortical neurons or enhanced fiber connectivity (Voss et al. 2014; Sampaio-Baptista and Johansen-Berg 2017). Myelination is the process by which myelin sheaths develop around nerve fibers, facilitating faster and more directed nerve conduction (Hartline and Colman 2007; Freeman et al. 2016). White matter measures, such as FA, AD, MD, and RD, are sensitive to the degree of myelination. Greater myelination, increased fiber density, and coherence of axon orientations contribute to decreased MD and RD and increased FA (Aboitiz et al. 1992; Song et al. 2002; Moura et al. 2016; Pohl et al. 2016). However, the tortuosity or straightening of axons influences the AD value (Joosten and Bar 1999; Takahashi et al. 2000; Giorgio et al. 2010; Brouwer et al. 2012). Previous studies on various diseases (Metwalli et al. 2010; Rosas et al. 2010; Salat et al. 2010; Della Nave et al. 2011; Zhang et al. 2016) have provided pathological evidence of these relationships, with higher diffusion measures corresponding to more severe atrophy in diseases. Abnormal increases in white matter diffusion are associated with abnormal myelination or demyelination (Song et al. 2005). Thus, in our study, the reduced white matter measures (i.e. AD, MD, and RD) observed in blind children relative to sighted controls reflect myelination changes in the rIFOF and FM during childhood. However, in adulthood, there were minimal or no differences between the two adult groups, suggesting cognitive functional reorganization of these tracts in adulthood. From childhood to adulthood, the reduction in white matter measures in sighted individuals reflected both the maturation of white matter clusters in the rIFOF and FM accompanied by the myelination of intracortical neurons during development. However, there were no differences in any of the measures between the two blind groups, and the values were very small, suggesting that the myelination of the rIFOF and FM had occurred in childhood and that these tracts were able to be cognitively functionally reorganized.

Our findings align with previous studies conducted on animals and humans, which also demonstrated plastic structural changes in the IFOF and FM (as the posterior segment of the CC) in blind adults (Yu et al. 2007; Bock et al. 2013; Tomaiuolo et al. 2014). Moreover, our study contributes by elucidating the developmental trajectory of the IFOF and FM from childhood to adulthood and highlights the crucial role of myelination in this process.

Cross-modal cognitive functional plasticity of the occipital structural network

We observed that long-term blindness resulted in a correlation between the structural values of the occipital cortex regions and the performance of tactile perception task. These findings are consistent with previous studies that have revealed the participation of the occipital cortices in blind individuals' auditory and tactile perception (Burton et al. 2004; Hötting and Röder 2009; Gagnon et al. 2010; Kupers et al. 2010; Collignon et al. 2011; Dormal et al. 2016), braille reading (Sadato et al. 1996; Hamilton et al. 2000; Burton et al. 2002, 2012), language processing (Amedi et al. 2004; Bedny et al. 2011, 2015; Striem-Amit et al. 2012; Watkins et al. 2012), and mathematics (Kanjlia et al. 2016).

In addition, our study suggested that long-term blindness led to a correlation between lFM and rFM tracts and braille reading abilities. The FM tract is a white matter pathway that connects the occipital lobes and crosses the midline through the splenium of the CC. Previous research has identified associations between the FM tracts and various cognitive functions in sighted individuals, including topographical orientation (Tamura et al. 2007), delayed memory (Liu et al. 2021), and face recognition (Thomas et al. 2009). Moreover, studies have demonstrated that damage to the FM tract can lead to reading disorders in sighted individuals (Damasio and Damasio 1983; Binder and Mohr 1992).

The posterior occipital regions and FM tracts in the blind transition from non-involvement in tactile perception and braille reading during childhood to undergoing cognitive functional reorganization during adulthood, participating in tactile perception and braille reading processing.

Regrettably, we did not find a correlation between these two tracts and visual word reading performance in our sighted subjects. These null results may be due to insufficient sensitivity of our word reading task in sighted individuals or the possibility that the involvement of FM tracts in reading may only manifest in abnormal conditions, such as brain lesions or visual deprivation. Nevertheless, our study is the first to observe the contribution of FM tracts to braille reading in congenitally blind adults. This suggests that long-term blindness leads to the recruitment of these tracts for tactile word reading.

Limitations

This study has several limitations to acknowledge. First, the sample size of blind children was small, due to recruitment challenges associated with the low incidence of congenital blindness. Second, the subjects in different age groups were not the same, indicating that this study did not have a longitudinal design. Third, our focus was solely on the interactive effects of age and vision, without considering the main effects. Fourth, we observed a dissociation between reading real words and nonwords in blind adults, and the underlying mechanisms need to be fully explored in future studies. Fifth, the way of stimulus presentation in the primary sensory perception task was not consistent in different vision groups, which should be addressed in future researches. Sixth, the blind subjects in this study were congenitally blind individuals with no variability in the age of blindness onset. Consequently, there was a lack of investigating the influence of the blindness onset on the reorganization of the occipital structural network in blindness. Last, it should be noted that the blind adults had a lower educational level than the sighted adults, which could have potentially confounded the observed developmental differences.

Conclusion

In conclusion, this study provided insights into the developmental reorganization of the structural network in the occipital cortex resulting from congenital blindness. From childhood to adulthood, blind individuals exhibited significant developmental changes in the occipital anatomical structures (specific regions and connections) relative to sighted individuals, along with cognitive functional reorganization in certain structures. Specifically, the posterior occipital regions (lCAL and rMOG) were involved in tactile perception, and the FM participated in braille reading in blind adults. These structural and cognitive

functional plastic changes due to visual deprivation may be attributed to experience-dependent neuronal apoptosis, pruning, or myelination.

Acknowledgments

We extend our gratitude to the participants for their involvement and to the members of BNU-CNLab for their significant contributions to data collection.

Authors' contributions

Saiyi Jiao (Conceptualization, Data curation, Formal analysis, Investigation, Visualization, Writing—original draft, Writing—review & editing), Ke Wang (Conceptualization, Data curation, Formal analysis, Investigation), Linjun Zhang (Data curation, Investigation), Yudan Luo (Data curation, Formal analysis), Junfeng Lin (Data curation, Formal analysis), and Zaizhu Han (Conceptualization, Formal analysis, Funding acquisition, Investigation, Supervision, Writing—review & editing).

Funding

This work was supported by the National Natural Science Foundation of China (32271091, 81870833, 81972144 and 82372555) and the National Defense Basic Scientific Research Program of China (2018YFC1315200).

Conflict of interest statement: None declared.

Data availability

Data will be available from the corresponding author upon reasonable request.

References

Aboitiz F, Scheibel AB, Fisher RS, Zaidel E. Fiber composition of the human corpus callosum. *Brain Res*. 1992:598(1–2):143–153.

Aguirre GK, Datta R, Benson NC, Prasad S, Jacobson SG, Cideciyan AV, Bridge H, Watkins KE, Butt OH, Dain AS, et al. Patterns of individual variation in visual pathway structure and function in the sighted and blind. *PLoS One*. 2016:11(11):e0164677.

Amedi A, Floel A, Knecht S, Zohary E, Cohen LG. Transcranial magnetic stimulation of the occipital pole interferes with verbal processing in blind subjects. *Nat Neurosci*. 2004:7(11):1266–1270.

Anurova I, Renier LA, De Volder AG, Carlson S, Rauschecker JP. Relationship between cortical thickness and functional activation in the early blind. *Cereb Cortex*. 2015:25(8):2035–2048.

Araneda R, Renier LA, Rombaux P, Cuevas I, De Volder AG. Cortical plasticity and olfactory function in early blindness. *Front Syst Neurosci*. 2016:10:75.

Ashburner J. A fast diffeomorphic image registration algorithm. *NeuroImage*. 2007:38(1):95–113.

Ashburner J, Friston KJ. Voxel-based morphometry—the methods. *NeuroImage*. 2000:11(6):805–821.

Barnes J, Ridgway GR, Bartlett J, Henley SMD, Lehmann M, Hobbs N, Clarkson MJ, MacManus DG, Ourselin S, Fox NC. Head size, age and gender adjustment in MRI studies: a necessary nuisance? *NeuroImage*. 2010:53(4):1244–1255.

Baron J, Strawson C. Use of orthographic and word-specific knowledge in reading words aloud. *J Exp Psychol Hum Percept Perform*. 1976:2:386–393.

Bedny M, Pascual-Leone A, Dodell-Feder D, Fedorenko E, Saxe R. Language processing in the occipital cortex of congenitally blind adults. *Proc Natl Acad Sci U S A*. 2011:108(11):4429–4434.

Bedny M, Richardson H, Saxe R. "Visual" cortex responds to spoken language in blind children. *J Neurosci*. 2015:35(33):11674–11681.

Binder JR, Mohr JP. The topography of callosal reading pathways. *Brain*. 1992:115(12):1807–1826.

Bock AS, Saenz M, Tungaraza R, Boynton GM, Bridge H, Fine I. Visual callosal topography in the absence of retinal input. *NeuroImage*. 2013:81:325–334.

Bridge H, Cowey A, Ragge N, Watkins K. Imaging studies in congenital anophthalmia reveal preservation of brain architecture in"visual" cortex. *Brain*. 2009:132(12):3467–3480.

Brouwer RM, Mandl RCW, Schnack HG, van Soelen ILC, van Baal GC, Peper JS, Kahn RS, Boomsma DI, Pol HEH. White matter development in early puberty: a longitudinal volumetric and diffusion tensor imaging twin study. *PLoS One*. 2012:7(4):e32316.

Burton H, Snyder AZ, Conturo TE, Akbudak E, Ollinger JM, Raichle ME. Adaptive changes in early and late blind: a fMRI study of braille reading. *J Neurophysiol*. 2002:87(1):589–607.

Burton H, Sinclair RJ, McLaren DG. Cortical activity to vibrotactile stimulation: an fMRI study in blind and sighted individuals. *Hum Brain Mapp*. 2004:23(4):210–228.

Burton H, Sinclair RJ, Agato A. Recognition memory for braille or spoken words: an fMRI study in early blind. *Brain Res*. 2012:1438:22–34.

Collignon O, Vandewalle G, Voss P, Albouy G, Charbonneau G, Lassonde M, Lepore F. Functional specialization for auditory–spatial processing in the occipital cortex of congenitally blind humans. *Proc Natl Acad Sci U S A*. 2011:108(11):4435–4440.

Cui Z, Zhong S, Xu P, He Y, Gong G. PANDA: a pipeline toolbox for analyzing brain diffusion images. *Front Hum Neurosci*. 2013:7:42.

Damasio AR, Damasio H. The anatomic basis of pure alexia. *Neurology*. 1983:33(12):1573–1573.

Della Nave R, Ginestroni A, Diciotti S, Salvatore E, Soricelli A, Mascalchi M. Axial diffusivity is increased in the degenerating superior cerebellar peduncles of Friedreich's ataxia. *Neuroradiology*. 2011:53(5):367–372.

Dillon CM, Pisoni DB. Nonword repetition and reading in deaf children with cochlear implants. *Int Congr Ser*. 2004:1273:304–307.

Dormal G, Rezk M, Yakobov E, Lepore F, Collignon O. Auditory motion in the sighted and blind: early visual deprivation triggers a large-scale imbalance between auditory and "visual" brain regions. *NeuroImage*. 2016:134:630–644.

Draganski B, Gaser C, Kempermann G, Kuhn HG, Winkler J, Buchel C, May A. Temporal and spatial dynamics of brain structure changes during extensive learning. *J Neurosci*. 2006:26(23):6314–6317.

Forster KI, Forster JC. DMDX: a Windows display program with millisecond accuracy. *Behav Res Methods Instrum Comput*. 2003:35(1):116–124.

Freeman SA, Desmazières A, Fricker D, Lubetzki C, Sol-Foulon N. Mechanisms of sodium channel clustering and its influence on axonal impulse conduction. *Cell Mol Life Sci*. 2016:73(4):723–735.

Gagnon L, Kupers R, Schneider FC, Ptito M. Tactile maze solving in congenitally blind individuals. *Neuroreport*. 2010:21(15):989–992.

Gaser C, Schlaug G. Brain structures differ between musicians and non-musicians. *J Neurosci*. 2003:23(27):9240–9245.

Giedd JN, Blumenthal J, Jeffries NO, Castellanos FX, Liu H, Zijdenbos A, Paus T, Evans AC, Rapoport JL. Brain development during childhood and adolescence: a longitudinal MRI study. *Nat Neurosci*. 1999:2(10):861–863.

Giorgio A, Watkins KE, Chadwick M, James S, Winmill L, Douaud G, De Stefano N, Matthews PM, Smith SM, Johansen-Berg H,

et al. Longitudinal changes in grey and white matter during adolescence. *NeuroImage*. 2010:49(1):94–103.
Gogtay N, Giedd JN, Lusk L, Hayashi KM, Greenstein D, Vaituzis AC, Nugent TF, Herman DH, Clasen LS, Toga AW, et al. Dynamic mapping of human cortical development during childhood through early adulthood. *Proc Natl Acad Sci U S A*. 2004:101(21):8174–8179.
Goldszal AF, Davatzikos C, Pham DL, Yan MXH, Bryan RN, Resnick SM. An image-processing system for qualitative and quantitative volumetric analysis of brain images. *J Comput Assist Tomogr*. 1998:22(5):827–837.
Goswami U, Ziegler JC, Dalton L, Schneider W. Nonword reading across orthographies: how flexible is the choice of reading units? *Appl Psycholinguist*. 2003:24(2):235–247.
Greenberg D, Ehri LC, Perin D. Do adult literacy students make the same word-reading and spelling errors as children matched for word-reading age? *Sci Stud Read*. 2002:6(3):221–243.
Greenough WT, Black JE, Wallace CS. Experience and brain development. *Child Dev*. 1987:58(3):539.
Griffiths YM, Snowling MJ. Predictors of exception word and nonword reading in dyslexic children: the severity hypothesis. *J Educ Psychol*. 2002:94(1):34–43.
Groeschel S, Vollmer B, King MD, Connelly A. Developmental changes in cerebral grey and white matter volume from infancy to adulthood. *Int J Dev Neurosci*. 2010:28(6):481–489.
Hamilton R, Keenan JP, Catala M, Pascual-Leone A. Alexia for braille following bilateral occipital stroke in an early blind woman. *Neuroreport*. 2000:11(2):237–240.
Hartline DK, Colman DR. Rapid conduction and the evolution of giant axons and myelinated fibers. *Curr Biol*. 2007:17(1):R29–R35.
Hötting K, Röder B. Auditory and auditory-tactile processing in congenitally blind humans. *Hear Res*. 2009:258(1–2):165–174.
Hu C-F, Catts HW. The role of phonological processing in early reading ability: what we can learn from Chinese. *Sci Stud Read*. 1998:2(1):55–79.
Hua K, Zhang J, Wakana S, Jiang H, Li X, Reich DS, Calabresi PA, Pekar JJ, van Zijl PCM, Mori S. Tract probability maps in stereotaxic spaces: analyses of white matter anatomy and tract-specific quantification. *NeuroImage*. 2008:39(1):336–347.
Jiang J, Zhu W, Shi F, Liu Y, Li J, Qin W, Li K, Yu C, Jiang T. Thick visual cortex in the early blind. *J Neurosci*. 2009:29(7):2205–2211.
Jiang A, Tian J, Li R, Liu Y, Jiang T, Qin W, Yu C. Alterations of regional spontaneous brain activity and gray matter volume in the blind. *Neural Plast*. 2015:2015:141950.
Joosten EAJ, Bar DPR. Axon guidance of outgrowing corticospinal fibres in the rat. *J Anat*. 1999:194(1):15–32.
Kanjlia S, Lane C, Feigenson L, Bedny M. Absence of visual experience modifies the neural basis of numerical thinking. *Proc Natl Acad Sci U S A*. 2016:113(40):11172–11177.
Kolb B. Age, experience and the changing brain. *Neurosci Biobehav Rev*. 1998:22(2):143–159.
Kolb B, Whishaw IQ. Brain plasticity and behavior. *Annu Rev Psychol*. 1998:49(1):43–64.
Kupers R, Chebat DR, Madsen KH, Paulson OB, Ptito M, Mishkin M. Neural correlates of virtual route recognition in congenital blindness. *Proc Natl Acad Sci U S A*. 2010:107(28):12716–12721.
Lenroot RK, Gogtay N, Greenstein DK, Wells EM, Wallace GL, Clasen LS, Blumenthal JD, Lerch J, Zijdenbos AP, Evans AC, et al. Sexual dimorphism of brain developmental trajectories during childhood and adolescence. *NeuroImage*. 2007:36(4):1065–1073.
Levin N, Dumoulin SO, Winawer J, Dougherty RF, Wandell BA. Cortical maps and white matter tracts following long period of visual deprivation and retinal image restoration. *Neuron*. 2010:65(1):21–31.
Li Q, Song M, Xu J, Qin W, Yu C, Jiang T. Cortical thickness development of human primary visual cortex related to the age of blindness onset. *Brain Imaging Behav*. 2017:11(4):1029–1036.
Lin J, Zhang L, Guo R, Jiao S, Song X, Feng S, Wang K, Li M, Luo Y, Han Z. The influence of visual deprivation on the development of the thalamocortical network: evidence from congenitally blind children and adults. *NeuroImage*. 2022:264:119722.
Liu Z, Kang L, Zhang A, Yang C, Liu M, Wang J, Liu P, Zhang K, Sun N. Injuries in left corticospinal tracts, forceps major, and left superior longitudinal fasciculus (temporal) as the quality indicators for major depressive disorder. *Neural Plast*. 2021:2021:2348072.
Maller JJ, Thomson RH, Ng A, Mann C, Eager M, Ackland H, Fitzgerald PB, Egan G, Rosenfeld JV. Brain morphometry in blind and sighted subjects. *J Clin Neurosci*. 2016:33:89–95.
Mandonnet E, Duffau H. Setting the balance between the lexical and sublexical pathways of dual-route models of reading: insight from atypical dyslexia in surgical glioma patients. *Front Psychol*. 2016:7:1730.
McKenzie IA, Ohayon D, Li H, Paes de Faria J, Emery B, Tohyama K, Richardson WD. Motor skill learning requires active central myelination. *Science*. 2014:346(6207):318–322.
Mechelli A, Crinion JT, Noppeney U, O'Doherty J, Ashburner J, Frackowiak RS, Price CJ. Structural plasticity in the bilingual brain. *Nature*. 2004:431(7010):757–757.
Metwalli NS, Benatar M, Nair G, Usher S, Hu X, Carew JD. Utility of axial and radial diffusivity from diffusion tensor MRI as markers of neurodegeneration in amyotrophic lateral sclerosis. *Brain Res*. 2010:1348:156–164.
Mills KL, Goddings A-L, Herting MM, Meuwese R, Blakemore S-J, Crone EA, Dahl RE, Güroğlu B, Raznahan A, Sowell ER, et al. Structural brain development between childhood and adulthood: convergence across four longitudinal samples. *NeuroImage*. 2016:141:273–281.
Mori S, van Zijl PCM. Fiber tracking: principles and strategies - a technical review. *NMR Biomed*. 2002:15(7–8):468–480.
Mori S, Crain BJ, Chacko VP, Van Zijl PCM. Three-dimensional tracking of axonal projections in the brain by magnetic resonance imaging. *Ann Neurol*. 1999:45(2):265–269.
Moura LM, Kempton M, Barker G, Salum G, Gadelha A, Pan PM, Hoexter M, Del Aquilla MAG, Picon FA, Anés M, et al. Age-effects in white matter using associated diffusion tensor imaging and magnetization transfer ratio during late childhood and early adolescence. *Magn Reson Imaging*. 2016:34(4):529–534.
Noppeney U, Friston KJ, Ashburner J, Frackowiak R, Price CJ. Early visual deprivation induces structural plasticity in gray and white matter. *Curr Biol*. 2005:15(13):R488–R490.
Oldfield RC. The assessment and analysis of handedness: the Edinburgh inventory. *Neuropsychologia*. 1971:9(1):97–113.
Olulade OA, Flowers DL, Napoliello EM, Eden GF. Developmental differences for word processing in the ventral stream. *Brain Lang*. 2013:125(2):134–145.
Pan W-J, Wu G, Li C-X, Lin F, Sun J, Lei H. Progressive atrophy in the optic pathway and visual cortex of early blind Chinese adults: a voxel-based morphometry magnetic resonance imaging study. *NeuroImage*. 2007:37(1):212–220.
Park H-J, Lee JD, Kim EY, Park B, Oh M-K, Lee S, Kim J-J. Morphological alterations in the congenital blind based on the analysis of cortical thickness and surface area. *NeuroImage*. 2009:47(1):98–106.
Peelle JE, Cusack R, Henson RNA. Adjusting for global effects in voxel-based morphometry: gray matter decline in normal aging. *NeuroImage*. 2012:60(2):1503–1516.
Pell GS, Briellmann RS, Patrick Chan CH, Pardoe H, Abbott DF, Jackson GD. Selection of the control group for VBM analysis: influence

of covariates, matching and sample size. *NeuroImage*. 2008:41(4): 1324–1335.

Pohl KM, Sullivan EV, Rohlfing T, Chu W, Kwon D, Nichols BN, Zhang Y, Brown SA, Tapert SF, Cummins K, et al. Harmonizing DTI measurements across scanners to examine the development of white matter microstructure in 803 adolescents of the NCANDA study. *NeuroImage*. 2016:130:194–213.

Ptito M, Schneider FCG, Paulson OB, Kupers R. Alterations of the visual pathways in congenital blindness. *Exp Brain Res*. 2008: 187(1):41–49.

Rakic P. Neurogenesis in adult primate neocortex: an evaluation of the evidence. *Nat Rev Neurosci*. 2002:3(1):65–71.

Raznahan A, Shaw P, Lalonde F, Stockman M, Wallace GL, Greenstein D, Clasen L, Gogtay N, Giedd JN. How does your cortex grow? *J Neurosci*. 2011:31(19):7174–7177.

Reislev NL, Kupers R, Siebner HR, Ptito M, Dyrby TB. Blindness alters the microstructure of the ventral but not the dorsal visual stream. *Brain Struct Funct*. 2016:221(6):2891–2903.

Riddoch MJ, Humphreys GW. *BORB: Birmingham object recognition battery*. Hove: Lawrence Erlbaum; 1993

Rosas HD, Lee SY, Bender AC, Zaleta AK, Vangel M, Yu P, Fischl B, Pappu V, Onorato C, Cha J-H, et al. Altered white matter microstructure in the corpus callosum in Huntington's disease: implications for cortical disconnection. *NeuroImage*. 2010:49(4): 2995–3004.

Sadato N, Pascual-Leone A, Grafman J, Ibañez V, Deiber M-P, Dold G, Hallett M. Activation of the primary visual cortex by braille reading in blind subjects. *Nature*. 1996:380(6574): 526–528.

Salat DH, Tuch DS, van der Kouwe AJW, Greve DN, Pappu V, Lee SY, Hevelone ND, Zaleta AK, Growdon JH, Corkin S, et al. White matter pathology isolates the hippocampal formation in Alzheimer's disease. *Neurobiol Aging*. 2010:31(2):244–256.

Sampaio-Baptista C, Johansen-Berg H. White matter plasticity in the adult brain. *Neuron*. 2017:96(6):1239–1251.

Sampaio-Baptista C, Khrapitchev AA, Foxley S, Schlagheck T, Scholz J, Jbabdi S, DeLuca GC, Miller KL, Taylor A, Thomas N, et al. Motor skill learning induces changes in white matter microstructure and myelination. *J Neurosci*. 2013:33(50):19499–19503.

Scholz J, Klein MC, Behrens TEJ, Johansen-Berg H. Training induces changes in white-matter architecture. *Nat Neurosci*. 2009:12(11): 1370–1371.

Shimony JS, Burton H, Epstein AA, McLaren DG, Sun SW, Snyder AZ. Diffusion tensor imaging reveals white matter reorganization in early blind humans. *Cereb Cortex*. 2006:16(11):1653–1661.

Shu N, Li J, Li K, Yu C, Jiang T. Abnormal diffusion of cerebral white matter in early blindness. *Hum Brain Mapp*. 2009:30(1): 220–227.

Song S-K, Sun S-W, Ramsbottom MJ, Chang C, Russell J, Cross AH. Dysmyelination revealed through MRI as increased radial (but unchanged axial) diffusion of water. *NeuroImage*. 2002:17(3): 1429–1436.

Song S-K, Yoshino J, Le TQ, Lin S-J, Sun S-W, Cross AH, Armstrong RC. Demyelination increases radial diffusivity in corpus callosum of mouse brain. *NeuroImage*. 2005:26(1):132–140.

Striem-Amit E, Cohen L, Dehaene S, Amedi A. Reading with sounds: sensory substitution selectively activates the visual word form area in the blind. *Neuron*. 2012:76(3):640–652.

Takahashi M, Ono J, Harada K, Maeda M, Hackney DB. Diffusional anisotropy in cranial nerves with maturation: quantitative evaluation with diffusion MR imaging in rats. *Radiology*. 2000:216(3): 881–885.

Tamura I, Kitagawa M, Otsuki M, Kikuchi S, Tashiro K, Dubois B. Pure topographical disorientation following a right forceps major of the splenium lesion: a case study. *Neurocase*. 2007:13(3):178–184.

Thomas C, Avidan G, Humphreys K, Jung K, Gao F, Behrmann M. Reduced structural connectivity in ventral visual cortex in congenital prosopagnosia. *Nat Neurosci*. 2009:12(1):29–31.

Tomaiuolo F, Campana S, Collins DL, Fonov VS, Ricciardi E, Sartori G, Pietrini P, Kupers R, Ptito M. Morphometric changes of the corpus callosum in congenital blindness. *PLoS One*. 2014:9(9):e107871.

Townsend JT, Ashby FG. *Stochastic modeling of elementary psychological processes*. London: Cambridge University Press; 1983.

Tzourio-Mazoyer N, Landeau B, Papathanassiou D, Crivello F, Etard O, Delcroix N, Mazoyer B, Joliot M. Automated anatomical labeling of activations in SPM using a macroscopic anatomical parcellation of the MNI MRI single-subject brain. *NeuroImage*. 2002:15(1): 273–289.

Vigneau M, Jobard G, Mazoyer B, Tzourio-Mazoyer N. Word and non-word reading: what role for the Visual Word Form Area? *NeuroImage*. 2005:27(3):694–705.

Voss P, Zatorre RJ. Occipital cortical thickness predicts performance on pitch and musical tasks in blind individuals. *Cereb Cortex*. 2012:22(11):2455–2465.

Voss P, Pike BG, Zatorre RJ. Evidence for both compensatory plastic and disuse atrophy-related neuroanatomical changes in the blind. *Brain*. 2014:137(4):1224–1240.

Wang R, Benner T, Sorensen AG, Wedeen VJ. Diffusion toolkit: a software package for diffusion imaging data processing and tractography. *Proc Intl Soc Mag Reson Med*. 2007:15:3720.

Watkins KE, Cowey A, Alexander I, Filippini N, Kennedy JM, Smith SM, Ragge N, Bridge H. Language networks in anophthalmia: maintained hierarchy of processing in "visual" cortex. *Brain*. 2012:135(5):1566–1577.

Wong M, Gnanakumaran V, Goldreich D. Tactile spatial acuity enhancement in blindness: evidence for experience-dependent mechanisms. *J Neurosci*. 2011:31(19):7028–7037.

Xia Y, Xia M, Liu J, Liao X, Lei T, Liang X, Zhao T, Shi Z, Sun L, Chen X, et al. Development of functional connectome gradients during childhood and adolescence. *Sci Bull*. 2022:67(10):1049–1061.

Yang C, Wu S, Lu W, Bai Y, Gao H. Anatomic differences in early blindness: a deformation-based morphometry MRI study: anatomic differences in early blindness using DBM. *J Neuroimaging*. 2014:24(1):68–73.

Yu C, Shu N, Li J, Qin W, Jiang T, Li K. Plasticity of the corticospinal tract in early blindness revealed by quantitative analysis of fractional anisotropy based on diffusion tensor tractography. *NeuroImage*. 2007:36(2):411–417.

Zhang Y, Wu I-W, Tosun D, Foster E, Schuff N, Parkinson's Progression Markers Initiative. Progression of regional microstructural degeneration in Parkinson's disease: a multicenter diffusion tensor imaging study. *PLoS One*. 2016:11(10):e0165540.

Zhao C, Yang L, Xie S, Zhang Z, Pan H, Gong G. Hemispheric module-specific influence of the X chromosome on white matter connectivity: evidence from girls with Turner syndrome. *Cereb Cortex*. 2019:29(11):4580–4594.